Studies on Structure and Electrocatalytic Hydrogen Evolution of Nanocrystalline Ni-Mo-Fe Alloy Electrodeposit Electrodes

HUANG, Ling* (黄令) **YANG, Fang-Zu**(杨防祖) **SUN, Shi-Gang**(孙世刚) **XU, Shu-Kai**(许书楷) **ZHOU, Shao-Min**(周绍民)

State Key Laboratory for Physical Chemistry on the Solid Surface, Department of Chemistry, Xiamen University, Xiamen, Fujian 361005, China

Nanocrystalline Ni-Mo-Fe alloy deposits were obtained by electrodeposition. The structures of the alloy deposits were analyzed by X-ray diffraction (XRD) and X-ray photoelectron spectroscopy (XPS). The XRD results of nanocrystalline Ni-Mo-Fe alloy deposit show that many diffraction lines disappear, and that there is only one diffraction peak at 44.0°. The XPS results of nanocrystalline Ni-Mo-Fe alloy deposits indicate that the nickel, molybdenum and iron of the deposits exist in metallic state, and that the binding energy of the alloyed elements increases to some extent. The nanocrystalline Ni-Mo-Fe alloy deposit electrode may offer better electrocatalytic activity than the polycrystalline nickel electrode and the nanocrystalline Ni-Mo alloy electrode. The electrochemical impedance spectra from the nanocrystalline Ni-Mo-Fe alloy electrode indicate that hydrogen evolution in 30% (*m/m*) KOH at lower overpotential is in accordance with the Volmer-Tafel mechanism, but with the Volmer-Heyrovsky mechanism at higher overpotential.

Keywords nanocrystalline Ni-Mo-Fe alloy, electrodeposition, structure and hydrogen evolution

Introduction

In order to reduce energy consumption for alkaline water electrolysis and chloralkali electrolysis, there have been numerous investigations on the preparation and electrocatalytic activity of electrode material for hydrogen evolution reaction (HER).[1,2] There are two main alternative methods to lower overvoltage for the HER: one is to increase the true electrode area by means of increasing the electrode roughness, and the other is to use electrocatalytically active alloy electrode. And a less common way to lower overvoltage of the HER is by changing the surface microstructure of alloy deposit electrodes.

Although the platinum group metals exhibit higher activity for hydrogen evolution,[3] the nickel-based alloy electrodes are also very active electrocatalyst for hydrogen evolution in alkaline media.[4,5] The Ni-based alloy electrode can be prepared by various methods such as sintering, vacuum or plasma sprayed deposition, or electrodeposition.[6-10] The electrodeposition method has advantages of simplicity and low cost, so it is often used to prepare electrocatalytic materials.

Although many researchers think that the electrocatalytic activity of the material depends on the surface roughness and type of the electrode material, there is controversy over the relationship between surface roughness and catalytic ability.[11]

Recently it has been shown that the nanocrystalline alloy with grain size less than 100 nm is a very promising electrocatalytically active material because of its special structure.[12,13] It is known that to deposit pure molybdenum in aqueous solution is impossible, but codeposition with iron-group metals is possible.[14] Previous researches indicate that nanocrystalline Ni-Mo alloy electrode has higher electrocatalytic activity for hydrogen evolution in alkaline media.[15] In this paper we report on the nanocrystalline Ni-Mo-Fe alloy deposit obtained by electrodeposition. X-Ray diffraction (XRD) and X-ray photoelectron spectroscopy (XPS) were used to study structural characteristics of nanocrystalline Ni-Mo-Fe alloy deposits, and the steady state polarization curves and AC impedance measurements were chosen to investigate the mechanism and electrocatalytic ability for hydrogen evolution on the Ni-Mo-Fe alloy deposit electrode in alkaline media.

Experimental

The Ni-Mo-Fe deposits were obtained from a solution containing $NiSO_4 \cdot 6H_2O$ (50 g/L), $Na_2MoO_4 \cdot 2H_2O$ (5—15 g/L), $K_4P_2O_7 \cdot 3H_2O$ (250 g/L), $FeSO_4 \cdot 7H_2O$ (20 g/L) and $Na_3C_6H_5O_7 \cdot 2H_2O$ (10 g/L) at pH 8.5 adjusted with $NH_3 \cdot H_2O$. Current density was 6 $A \cdot dm^{-2}$, temperature 30 ℃, and deposition time 30 min. The Ni-Mo-Fe alloy deposits were deposited on mild steel substrates, which were polished before use with cabinet sandpaper of decreasing grain size and

* E-mail: huangl@jingxian.xmu.edu.cn

Received May 15, 2002; revised November 4, 2002; accepted December 9, 2002.

Project supported by the National Natural Science Foundation of China (No. 20073037) and the Major State Basic Research Development Program (No. 2002CBZ 11800).

subsequently degreased with acetone, and then dipped into dilute $NH_3 \cdot H_2O$ solution for 3 min and finally into dilute HCl solution for 3 min. Their on-plating faces were insulated with insulating coating. The anode was a nickel sheet of high purity (99.99%).

The Ni, Fe and Mo contents of the deposits were determined by EDTA titration after dissolution. The X-ray diffraction (XRD) experiments were carried out on an X-ray rotating powder diffractometer of D/MAX-RC (Rigaku, Japan) with Cu Kα radiation, tube potential 40 kV, tube current 30 mA and scan rate 2 (°)/min.

The X-ray photoelectron spectroscopy (XPS) experiments were conducted on the ESCLABMKll X-photoelectron spectrometer using Mg Kα X-radiation, and the pass energy is 20 eV. The base pressure in the sample chamber varied from 1.33×10^{-6} to 1.33×10^{-7} $N \cdot m^{-2}$. Calibration was based upon the carbon 1s electron peak (284.6 eV) due to residual pump oil on the sample surface.

The steady state polarization curves were measured using a computer controlled EG&G (model 273) potentiostat. The M273 potentiostat and EG&G 5208 lock-in analyzer were used for the electrochemical impedance spectral measurements (EIS) controlled by an IBM XT-286 microcomputer. In the EIS measurements, the amplitude of the ac signal was 5 mV, and the frequency range was from 10 kHz to 1 Hz.

Electrochemical experiments were conducted with 0.5 cm^2 electrode in a three-compartment glass cell: the counter electrode was a 3 cm^2 platinum foil, with a Hg/HgO, 1 mol/L OH^- electrode as the reference electrode linked to the main compartment via a luggin capillary. The alkaline solution was prepared from analytical grade KOH in triply distilled water and was pre-electrolyzed in order to eliminate the electroactive impurities. Pre-electrolyzed alkaline solution was also purged with purified nitrogen prior to the experiments.

Results and discussion

X-*Ray diffraction results of the* Ni-Mo-Fe *alloy deposits*

The structures of the deposit were investigated by X-ray diffraction (XRD) analysis. The results are given in Fig. 1. From Fig. 1, it can be seen that many diffraction lines disappear, and there is only one diffraction peak at 44°. The Ni-Mo-Fe alloy deposit with Ni (68%), Mo (25%), Fe (7%) consists of face-centered cubic solid solution, with nickel as solvent, molybdenum and iron as solute. The broadening of diffraction line indicates that crystal lattice distortion is probably caused by codeposition of nickel, iron with molybdenum. After separating peaks and deducting line broadening, we can calculate the integral half with (111) line and grain size, *i.e.*, $\beta_{(111)}$ is 2.57°, grain size $D_{(111)}$ is 3.7 nm. This indicates that the crystalline grain size of the Ni-Mo-Fe alloy deposit is very small. But it has also been found that the diffraction peak shape of the Ni-Mo-Fe alloy deposit is different from the amorphous state alloy, so it should be considered as nanocrystailine.

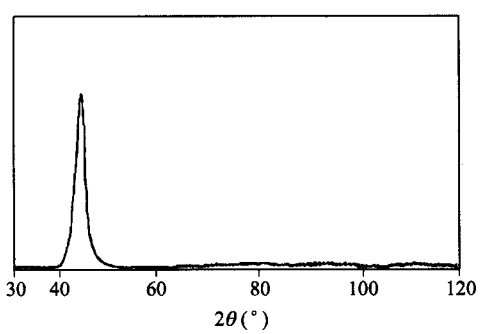

Fig. 1 XRD pattern of nanocrystalline Ni-Mo-Fe alloy deposit.

X-*Ray photoelectron energy spectral results of the* Ni-Mo-Fe *alloy deposits*

In order to determine the state of individual species in Ni-Mo-Fe alloy deposits, the structure of Ni-Mo-Fe alloy deposits was also analyzed by XPS. All samples of Ni-Mo-Fe alloy deposits were etched with argon ion for 60 s before the spectra were obtained. $Ni_{2p_{3/2}}$ XPS spectrum of Ni-Mo-Fe alloy deposits is given in Fig. 2. From Fig. 2, it can be seen that the nickel exists as metal in the deposit. The XPS spectrum of the Ni-Mo-Fe alloy deposit has a peak at binding energy 853.5 eV, which is assigned as $Ni_{2p_{3/2}}$ peak spectra referred to the standard XPS handbook,[16] but the binding energy has a displacement of 1.0 eV. This result indicates that the chemical circumstances of nickel atom have changed. Mo_{3d} XPS spectra of the Ni-Mo-Fe alloy deposits are given in Fig. 3. From Fig. 3, it can be found that the XPS spectra of Ni-Mo-Fe alloy deposit have the two peaks at binding energy 228.9 eV and 232.0 eV, assigned as the $3d_{5/2}$ and $3d_{3/2}$ peak of Mo(0) respectively. Spin-orbit splitting may cause the energy level splitting of Mo_{3d}, so the molybdenum exists as metallic molybdenum in the deposit, but the binding energy of Mo_{3d} in nanocrystalline Ni-Mo-Fe alloy has a displacement of 1.2 eV. This result shows that the chemical circumstances of the molybdenum atom have also changed.

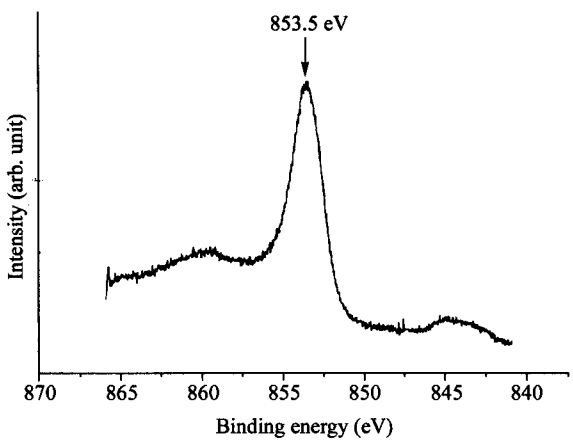

Fig. 2 XPS $Ni_{2p_{3/2}}$ spectrum of nanocrystalline Ni-Mo-Fe alloy deposit.

Fe_{2p} XPS spectrum of the Ni-Mo-Fe alloy deposits is given in Fig. 4. From Fig. 4, it can be found that the XPS spectrum of Ni-Mo-Fe alloy deposit has the two peaks at binding energy 708.4 eV and 721.0 eV, assigned as the 2p peak of Fe(0). Spin-orbit splitting may cause the energy level splitting of Fe_{2p}, so the iron exists as metallic iron in the deposit. But the binding energy of Fe_{2p} in nanocrystalline Ni-Mo-Fe alloy has a displacement of 0.9 eV. The surface atoms on the nanocrystalline Ni-Mo-Fe alloy possess higher reaction activity because of their high surface energy. The atom transfer and electron configuration on the surface of nanocrystalline Ni-Mo-Fe alloy deposit would be changed when crystal grain size of alloy deposit is very small. The change of atom transfer and electron configuration on the surface of nanocrystalline alloy may give rise to the binding energy displacement of the elements in the nanocrystalline deposit.[17] These results foretell that the nanocrystalline Ni-Mo-Fe alloy has specific electrochemical properties.

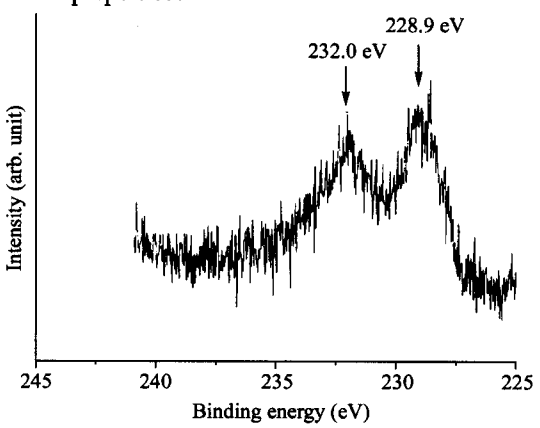

Fig. 3 Mo_{3d} XPS spectrum of nanocrystalline Ni-Mo-Fe alloy deposit.

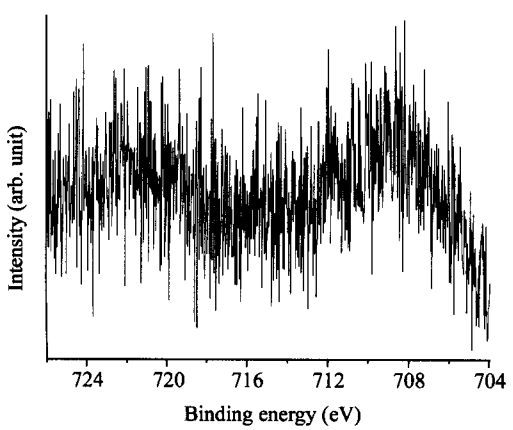

Fig. 4 Fe_{2p} XPS spectrum of nanocrystalline Ni-Mo-Fe alloy deposit.

Electrocatalytic activities of hydrogen evolution on the Ni-Mo-Fe *alloy deposit electrodes*

The steady-state polarization curve obtained on nanocrystalline Ni-Mo-Fe alloy electrode in 30 wt% KOH at 25 ℃ is given in Fig. 5. From Fig. 5, the overvoltage of hydrogen evolution on nanocrystalline Ni-Mo-Fe alloy electrodes at current density of 100 $mA \cdot cm^{-2}$ and the electrochemical parameters of the hydrogen evolution reaction can be calculated and tabulated in Table 1.

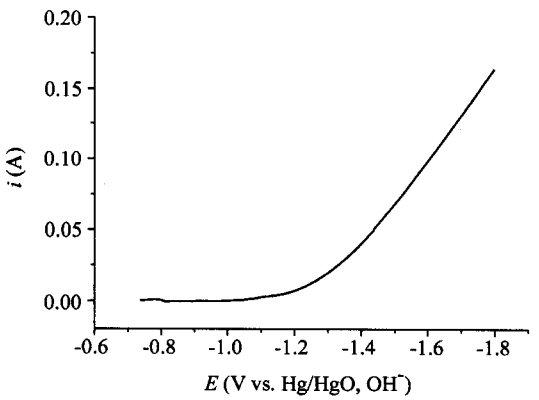

Fig. 5 Cathodic polarization curve of nanocrystalline Ni-Mo-Fe electrode in 30% KOH.

The electrochemical parameters of hydrogen evolution reaction were evaluated by linear regression analysis according to the relation:

$$\eta = -\frac{2.3RT}{\alpha nF}\lg i^0 + \frac{2.3RT}{\alpha nF}\lg i$$

The equation is simplified as

$$\eta = a + b\lg i$$

in which α represents the cathodic transfer factor, i^0 the exchange current density, and η the overpotential of hydrogen evolution reaction. From Table 1, it can be found that the overvoltage for the hydrogen evolution reaction on nanocrystalline Ni-Mo-Fe alloy deposit electrode is lower than that on nanocrystalline Ni-Mo electrode. The hydrogen evolution overpotential of nanocrystalline Ni-Mo-Fe alloy deposit electrode is lower by 22 mV than that of nanocrystalline Ni-Mo electrode. The exchange current density for hydrogen evolution on nanocrystalline Ni-Mo-Fe alloy deposit electrode is

Table 1 Electrochemical parameters of hydrogen evolution reaction on nanocrystalline Ni-Mo-Fe alloy electrode in 30% KOH

Electrode	a (mV)	b (mV)	α	i^0($A \cdot cm^{-2}$)	η (mV) (i = 100 $mA \cdot cm^{-2}$)
(1)	413	121	0.49	3.86×10^{-4}	517
(2)	472	185	0.32	2.80×10^{-4}	262
(3)	453.0	195.0	0.30	4.80×10^{-3}	240

(1) Polycrystalline Ni electrode[15]. (2) Nanocrystalline Ni-Mo alloy electrode[15]. (3) Nanocrystalline Ni-Mo-Fe alloy electrode.

seventeen times as large as that on nanocrystalline Ni-Mo alloy deposit electrode. Higher electrocatalytic activities of nanocrystalline Ni-Mo-Fe alloy deposit for hydrogen evolution may be related to the surface structure of Ni-Mo-Fe alloy because the molybdenum metal has a half-filled d-orbital, but the nickel and iron metal have unpaired d-electrons. When molybdenum codeposits with nickel and iron, the nanocrystalline Ni-Mo-Fe alloy has more d-electrons than the nanocrystalline Ni-Mo alloy deposit electrode. The electronic structure of the nanocrystalline Ni-Mo-Fe alloy is beneficial for proton combination and transfer. From XRD, the overpotential of hydrogen evolution becomes lower with the smaller size of crystalline grain because more crystal lattice defects and a larger crystal interface are presented by the smaller crystallites. The atoms at crystal lattice defects and dislocations are considered as active centers for the hydrogen evolution reaction, whereby the overpotential of hydrogen evolution reaction can be reduced. So the nanocrystalline Ni-Mo-Fe alloy deposit electrode has the lower overpotential of hydrogen evolution reaction.

AC *Impedance results of hydrogen evolution on nanocrystalline* Ni-Mo *alloy deposit electrode*

It is essential to investigate the mechanism of hydrogen evolution in alkaline media using ac impedance techniques, because there is an adsorption intermediate H_{ads} in the hydrogen evolution process.[2] Impedance spectra at the nanocrystalline Ni-Mo-Fe alloy deposit electrode in 30 wt% KOH at 25 ℃ are given in Fig. 6. It should be noted that two semicircles were observed on the Nyquist plots at lower applied potential, but one semicircle was observed on the Nyquist plots at higher applied potential. The smaller the radius of semicircle becomes, the higher the applied potential for hydrogen evolution. These results indicate that hydrogen evolution reaction on nanocrystalline Ni-Mo-Fe alloy deposit electrode at lower applied potential in 30 wt% KOH is in accordance with the Volmer-Tafel mechanism. The hydrogen evolution reaction on nanocrystalline Ni-Mo-Fe alloy deposit electrode in 30 wt% KOH involves an initial discharge of a water molecule, which is followed by a chemical desorption. At higher applied potential the mechanism of hydrogen evolution reaction on the alloy electrode is in accordance with the Volmer-Heyrovsky mechanism. The HER on the alloy deposit electrode involves an initial discharge of a water molecule, which is followed by an electrochemical desorption.

Conclusions

The electrocatalytically active Ni-Mo-Fe nanocrystalline alloy materials have been prepared by electrodeposition. XRD results of such Ni-Mo-Fe alloy deposits show that the grain size is very small. XPS results from nanocrystalline Ni-Mo-Fe alloy deposit indicate that the binding energy of the constituent metals is increased to some extent. The integral half height of the X-ray diffraction peak is related to the grain size and the constituent content of the alloy deposits. The catalytic performance of nanocrystalline Ni-Mo-Fe alloy for hydrogen evolution reaction is strongly dependent on the grain size and composition of the electrodes.

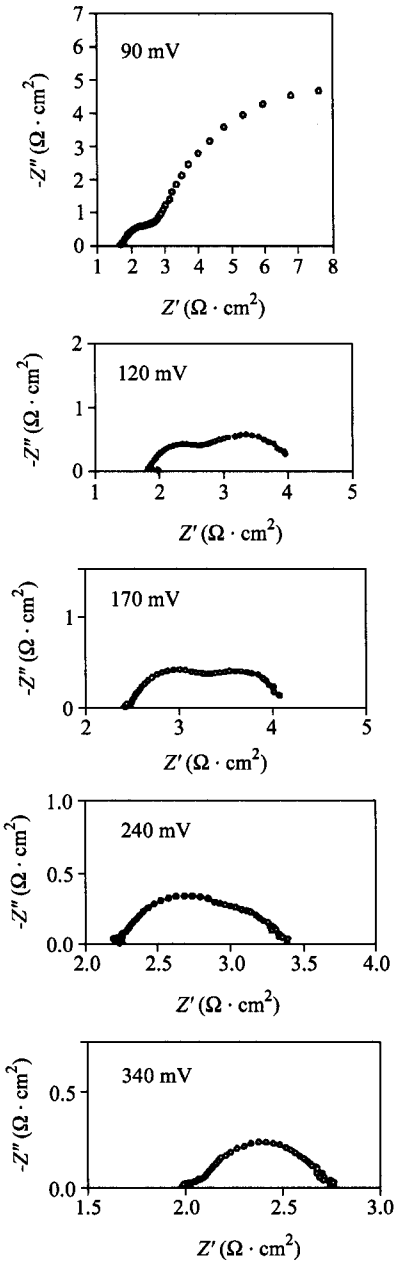

Fig. 6 EIS spectra for hydrogen evolution reaction on nanocrystalline Ni-Mo-Fe electrode.

References

1 Wendt, H.; Imarisio, G. *J. Appl. Electrochem.* **1988**, *18*, 1.
2 Divisek, J. *J. Electroanal. Chem.* **1986**, *214*, 615.
3 Kita, H. *J. Electrochem. Soc.* **1966**, *113*, 1095.
4 Bowen, G. T.; Davis, H. J.; Henshaw, B. F. *Int. J. Hydrogen Energy* **1984**, *9*, 59.
5 Loherberg, K.; Kohl, P. *Electrochim. Acta* **1984**, *29*, 1557.
6 Endoh, E.; Otonma, H.; Morimote, T.; Oda, Y. *Int. J. Hydrogen Energy* **1987**, *12*, 473.

7 Conway, B. E.; Kozlowska, H. A. ; Sattar, M. A. *J. Electrochem. Soc*. **1983**, *130*, 1825.
8 Brown, D. E.; Mahmood, M. N.; Man, M. C. M.; Turner, A. K. *Electrochim. Acta* **1984**, *29*, 1551.
9 Hall, D. E. *J. Appl. Electrochem*. **1984**, *14*, 107.
10 Conway, B. E.; Bai, L.; Tessier, D. F. *J. Electroanal. Chem*. **1984**, *161*, 39.
11 Yamashita, H.; Yamamura, T.; Yashimoto, K. *J. Electrochem. Soc*. **1993**, *140*, 2238.
12 Erb, U.; El-Sherik, A. M.; Palumbo, G.; Aust, K. T. *Nanostr. Mater*. **1993**, *2*, 383.
13 Huot, Y. J.; Trudeau, M. L.; Schulz, R. *J. Electrochem. Soc*. **1991**, *138*, 1316.
14 Brenner, A. *Electrodeposition of Alloys*, Vol. Ⅱ, Academic Press, New York, **1963**, p. 345.
15 Huang, L.; Yang, F. Z.; Xu, S. K.; Zhou, S. M. *Trans. Inst. Met. Finish*. **2001**, *79*, 136.
16 Wagner, C. D.; Riggs, W. M.; Davis, L. E.; Moulder, J. F. *Handbook of X-Ray Photoelectron Spectroscope*, Perkin-Elmer Corporation, Eden Prairie, Minnesota, **1979**.
17 Ball, P.; Garwin, L. *Nature* **1992**, *355*, 761.

(E0205156 PAN, B. F.; DONG, H. Z.)